Journal of Inflammation Research

Dovepress
Taylor & Francis Group

Open Access Full Text Article

ORIGINAL RESEARCH

Gegen Qinlian Decoction Mitigates DSS-Induced Acute Colitis and Reinstates Gut Barrier Function in Mice, Correlating with Suppressed IL-33/ST2 Signaling

Yuqi Wu[1,2,*], Mengqing Ma[3,*], Liuru Luo[4], Weijian Zhang[5], Xinxin Hong[5], Xiaoyan Jiang[5], Junyi Li[6], Sihui Zeng[2], Kexin Li[2], Huishan Yuan[2], Shaoju Guo[5], Lin Xu[5]

[1]Nanjing Hospital of Chinese Medicine Affiliated to Nanjing University of Chinese Medicine, Nanjing University of Chinese Medicine, Nanjing, Jiangsu, 210022, People's Republic of China; [2]The Fourth Clinical Medical College, Guangzhou University of Chinese Medicine, Shenzhen, Guangdong, 518033, People's Republic of China; [3]Department of Gastroenterology, Nanjing First Hospital, Nanjing Medical University, Nanjing, Jiangsu, 210006, People's Republic of China; [4]National Resource Center for Chinese Materia Medica, China Academy of Chinese Medical Sciences, Beijing, 100007, People's Republic of China; [5]Department of Gastroenterology, Shenzhen Traditional Chinese Medicine Hospital, The Fourth Clinical Medical College of Guangzhou University of Chinese Medicine, Shenzhen, Guangdong, 518033, People's Republic of China; [6]The Fifth Clinical Medical College, Guangzhou University of Chinese Medicine, Guangzhou, Guangdong, 510095, People's Republic of China

*These authors contributed equally to this work

Correspondence: Lin Xu; Shaoju Guo, Email 920xulin@sina.com; gsj1080@163.com

Background: As a classical prescription documented in the Treatise on Febrile Diseases, Gegen Qinlian Decoction (GGQLD) has been widely utilized for diarrhea and dysentery across history. Modern research indicates its potential efficacy in inflammatory bowel diseases, including ulcerative colitis (UC).

Aim: To elucidate the pathways involved, this research examined how GGQLD reduces the severity of DSS-induced colitis in mice.

Methods: To establish acute colitis, C57BL/6J mice were exposed to 3% DSS. Different doses of GGQLD, recombinant IL-33, or an IL-33-neutralizing antibody were then administered. The expression profiles of IL-33/ST2 pathway components and epithelial barrier proteins were investigated using immunostaining, qPCR, and Western blotting. Macrophage phenotypes were evaluated by flow cytometry, and cytokine secretion was assessed by ELISA.

Results: DSS exposure increased IL-33 expression, accompanied by a shift toward an M1-like macrophage phenotype and epithelial barrier damage. Recombinant IL-33 further exacerbated inflammation and permeability. In contrast, GGQLD and IL-33 neutralization alleviated colitis and reversed these changes. GGQLD treatment was accompanied by reduced M1-associated responses and an increased proportion of $CD163^{+}$ M2-like macrophages, together with decreased TNF-α and elevated IL-10 levels. In parallel, restoration of β-catenin and E-cadherin expression was observed, along with reduced ST2 expression.

Conclusion: In a DSS-induced acute colitis mouse model, GGQLD alleviated disease severity and reduced IL-33/ST2 signaling activity. In parallel, macrophages displayed a shift toward an M2-like phenotype, accompanied by changes in inflammatory cytokine profiles and improved intestinal epithelial barrier integrity. These findings suggest that modulation of the IL-33/ST2 pathway may be involved in the therapeutic effects of GGQLD.

Keywords: Gegen Qinlian Decoction, ulcerative colitis, IL-33/ST2 pathway, macrophage M2-like phenotype

Introduction

As a chronic inflammatory condition restricted to the colon, ulcerative colitis (UC) represents a key subtype of inflammatory bowel disease (IBD). In contrast, Crohn's disease (CD) may affect any segment of the gastrointestinal tract and exhibits discontinuous, transmural inflammation.[1,2] With a global prevalence approaching 5 million cases and a steadily increasing incidence, UC has emerged as a substantial public health burden. From a clinical perspective, the

https://doi.org/10.2147/JIR.S601288
Received: 16 February 2026
Accepted: 16 May 2026
Published: 10 July 2026

Graphical Abstract

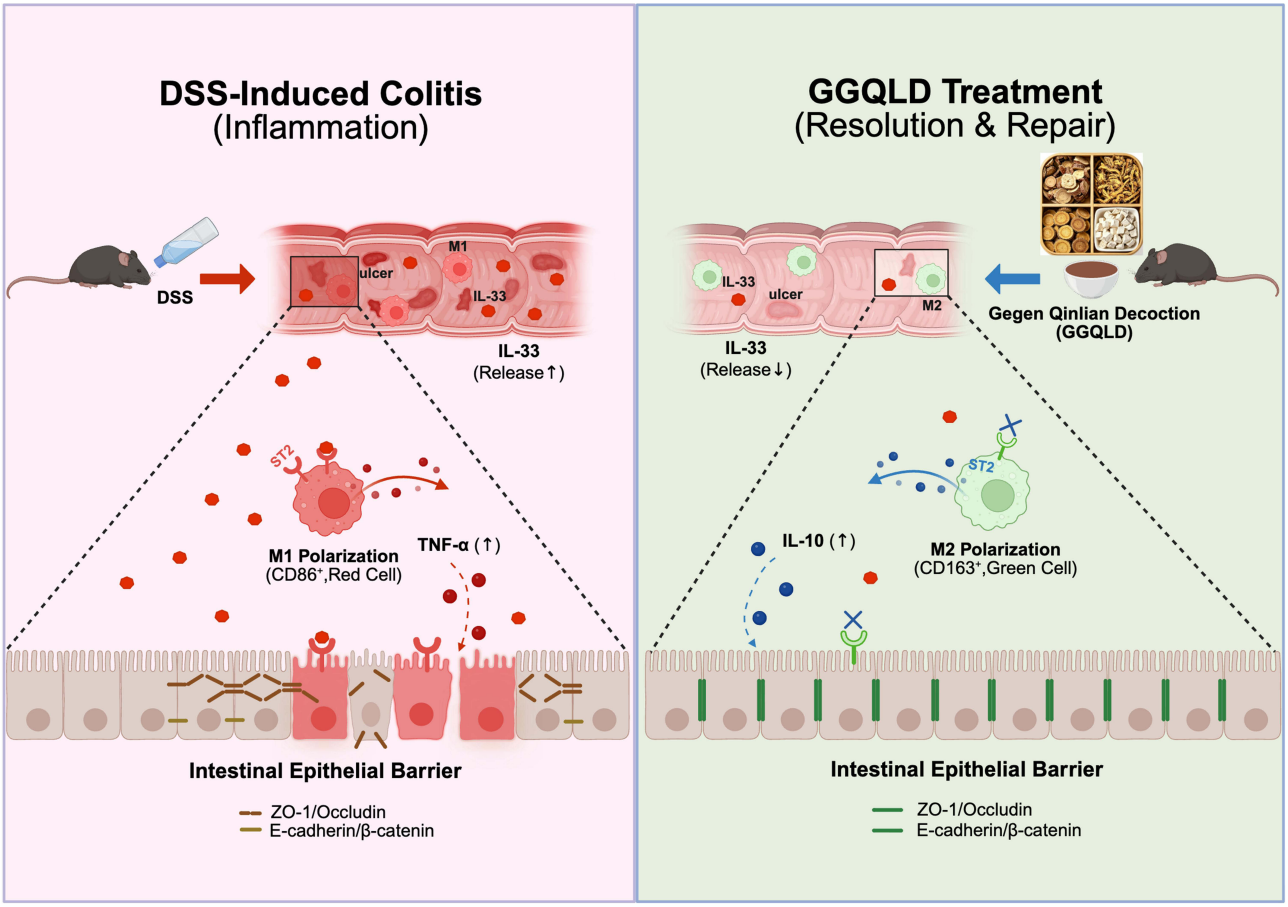

disease follows a recurrent course marked by alternating relapse and remission, and is commonly associated with bloody diarrhea, abdominal discomfort, and weight loss.[3–5] Although its underlying cause has not been completely defined, UC is considered a multifactorial disorder involving complex interactions between immune dysfunction, epithelial barrier disruption, and intestinal microbiota dysbiosis.[1,2,6–12] Impairment of epithelial junctional complexes—particularly proteins such as ZO-1, occludin, E-cadherin, and β-catenin—is considered a defining feature of barrier dysfunction in UC.[13,14]

Interleukin-33 (IL-33), a cytokine belonging to the IL-1 family, is constitutively expressed in epithelial and stromal compartments and released in response to tissue injury.[15,16] Elevated IL-33 levels have been consistently observed in inflamed mucosal tissues from UC patients.[17] Expressed by both epithelial and immune cell types, tumorigenicity 2 (ST2) functions as a key regulator of intestinal inflammatory responses.[18] Importantly, the IL-33/ST2 axis exerts context-dependent effects: under controlled conditions, it may facilitate epithelial repair, whereas excessive or sustained activation can exacerbate inflammation and barrier damage.[18–20] This duality underscores its complex involvement in mucosal homeostasis and disease progression.

In the intestinal immune system, macrophages serve critical regulatory functions and possess a high degree of functional adaptability. In UC, a skewed balance toward pro-inflammatory M1 macrophages, accompanied by insufficient M2-mediated repair responses, is frequently observed and contributes to chronic inflammation and defective mucosal healing.[21–26] Evidence indicates that the IL-33/ST2 axis may be associated with regulation of macrophage polarization in

a manner dependent on the specific context.[22,23] Therefore, therapeutic strategies aimed at restoring macrophage equilibrium, particularly by promoting M2-like phenotypes, have attracted increasing attention.[26,27]

Increasing evidence indicates that UC cannot be solely attributed to immune dysregulation, but rather arises from intricate interactions among epithelial barrier dysfunction, microbial dysbiosis, and aberrant immune activation. Accordingly, therapeutic approaches that simultaneously target inflammatory responses and gut microbiota alterations may provide synergistic benefits in reestablishing intestinal homeostasis, offering advantages over conventional immunosuppressive strategies.[28]

Gegen Qinlian Decoction (GGQLD), a classical traditional Chinese medicine formulation, has shown promising efficacy in the management of UC. Experimental studies have shown that GGQLD attenuates DSS-induced colitis, accompanied by improvements in inflammatory responses, epithelial barrier integrity, and gut microbiota composition.[29–33] Phytochemical analyses using UPLC-MS have identified several major constituents, among which puerarin, baicalin, and berberine are regarded as key bioactive components.[34] Notably, pharmacokinetic studies have indicated that puerarin and berberine preferentially accumulate in colonic tissues following oral administration, supporting their potential relevance in intestinal diseases.[35] These compounds are known to target critical pathogenic pathways in UC: puerarin inhibits NF-κB signaling and M1-like macrophage activation while influencing microbial metabolism;[36,37] baicalin contributes to epithelial barrier integrity and immune homeostasis via the AhR/IL-22 axis; and berberine has been reported to be associated with M2-like macrophage polarization and mucosal repair, potentially involving PPAR-γ-related mechanisms.[38–40]

Taken together, these findings indicate that GGQLD exerts multi-target regulatory effects involving immune responses, epithelial barrier function, and microbiota balance. However, whether its therapeutic benefits involve modulation of the IL-33/ST2 axis and macrophage phenotype-related changes in experimental colitis remains to be further clarified. Importantly, the DSS-induced acute colitis model mainly represents short-term epithelial injury and innate immune responses, and does not fully recapitulate the chronic, relapsing features characteristic of human ulcerative colitis.[41]

Experimental Procedures

Compounds and Sources

Dextran sulfate sodium (DSS; molecular weight: 36,000–50,000 Da; Cat. No. 216011080) was purchased from MP Biomedicals Inc. (Santa Ana, CA, USA). Recombinant Mouse IL-33 (carrier-free; Cat. No. 580508) was obtained from BioLegend (San Diego, CA, USA). The Mouse IL-33 Antibody (Cat. No. AF3626) was procured from R&D Systems (Minnesota, USA). Gegen Qinlian Decoction (GGQLD) was prepared by the Department of Pharmacy, Shenzhen Hospital of Traditional Chinese Medicine. The formula consists of *Pueraria lobata (Willd). Ohwi* (Gegen), *Scutellaria baicalensis Georgi* (Huangqin), *Coptis chinensis French* (Huanglian) and *Glycyrrhiza uralensis Fisch* (Gancao). To ensure taxonomic accuracy, the botanical names were checked and confirmed with reference to the World Flora Online database (http://www.worldfloraonline.org). The crude herbs were weighed and mixed in a ratio of 8:3:3:2, with a total weight of 48 g. The mixture underwent a 30-minute soak in distilled water prior to a 1-hour boiling period. The decoction was collected, and the residue was boiled once more with added distilled water for a further hour. Subsequently, the supernatant was subjected to concentration at 55 °C with a rotary evaporator (Xiande-2000A, Shanghai Xiande Experimental Instrument Co., Ltd., China) to extract with a density of 1.456 g/mL (crude drug equivalent). We prepared working solutions for analysis by diluting the stock solution with distilled water to obtain medium-dose (0.728 g/mL) and low-dose (0.304 g/mL) preparations for animal administration.

Uplc-Ms

Separation was carried out on a Waters Acuity UPLC HSS T3 column (100 × 2.1 mm, 1.8 μm) maintained at 40 °C, using a mobile phase of (A) acetonitrile and (B) 0.1% aqueous formic acid. For qualitative analysis, a gradient from 5% to 100% A over 35 min (0.35 mL/min; 3 μL injection) was applied. The quantitative gradient ran from 10% to 55% A over 16 min (0.35 mL/min; 2 μL injection). Following analysis, samples were analyzed on a Waters Xevo G2 Q-TOF

mass spectrometer coupled with an ESI source in both positive and negative ion modes (m/z 50–1200). Source conditions were: capillary voltage ±2.5 kV, cone voltage ±40 V, temperature 110 °C, with desolvation (N_2, 500 °C, 800 L/h) and cone (N_2, 50 L/h) gas flows.

Calibration: Leucine enkephalin was used for real-time lock mass correction. For qualitative analysis, a Fast DDA (data-dependent acquisition) method was applied, fragmenting the top 8 most intense precursor ions per cycle. The collision energy was set at 50 V for high mass and 25 V for low mass. A proprietary database containing 180 chemical constituents derived from literature and public databases of each single herb was established. Data processing was performed using UNIFI software for rapid component identification.

Animal Experiments

Male C57BL/6J mice aged 6–8 weeks were supplied by Zhuhai BesTest Bio-tech Co., Ltd. (Guangdong, China; Laboratory Animal Production License No. SCXK (Yue) 2020–0051; animal certificate No. 44822700038272). Animals were maintained in a specific pathogen-free environment at the Experimental Animal Center of Guangzhou University of Chinese Medicine (25 °C; 60 ± 5% humidity; 12-hour alternating light and dark periods) with free access to food and water. We provided a 7-day period for acclimatization before starting experiments. Approval for all animal procedures was granted by the Animal Ethics Committee of the School of Chinese Materia Medica, Guangzhou University of Chinese Medicine (Ethical Approval No. 20220302046; Date: March 3, 2022).

Induction and Therapies of Colitis

Upon completion of acclimatization, mice were weighed and randomly assigned to seven groups of eight each using SPSS 26.0 with a computer-generated random number table: Control (Con), DSS model (M), and Low-dose GGQLD (GL), Medium-dose GGQLD (GM), High-dose GGQLD (GH), IL-33 intervention (rmIL-33), and Anti-IL-33 intervention (ANTI IL-33) groups. The investigator performing data collection (including DAI scoring, colon length measurement, and histopathological evaluation) and statistical analysis was blinded to group allocation. 3% (w/v) DSS dissolved in drinking water was given to mice in all experimental groups freely for 7 days, thereby developing acute colitis. The Control group received normal drinking water throughout this period. Concurrently (days 1–7), treatment was administered as follows: The GL, GM, and GH groups received oral gavage of GGQLD at doses of 3.64, 7.28, and 14.56 g crude drug/kg/day, respectively. All GGQLD doses were diluted in distilled water. The IL-33 intervention group received daily i.p. administrations of Recombinant Mouse IL-33 (50 μg/kg/day),[42] diluted in PBS. The Anti-IL-33 intervention group received daily i.p. injections of Mouse IL-33 Antibody at 60 μg/kg/day),[43] diluted in PBS. Equivalent volumes of distilled water were given to the Control and DSS model groups to ensure consistency in gavage administration. At the study endpoint on day 7, all mice were euthanized by cervical dislocation under deep anesthesia with isoflurane (Figure 1A).

Disease Activity Index (DAI)

Mice were scored daily for DAI according to established criteria that drop in body weight, fecal consistency, and fecal bleeding. Body weight loss percentage was calculated relative to the initial weight. Stool samples were analyzed for bleeding with a commercial kit. The DAI was derived by averaging the scores (0–4 each) of three individual parameter scores, as specified in Table 1.

Spleen Weight Index

On the final day, the spleen was promptly harvested and weighed. Then, we calculated the index (spleen weight/body weight × 100%).

Histological Analysis

We collected a 2.0 cm distal colon segment, fixed it in 4% paraformaldehyde, and subsequently processed it through graded ethanol and xylene prior to paraffin embedding. From these blocks, 4 μm-thick sections were obtained and

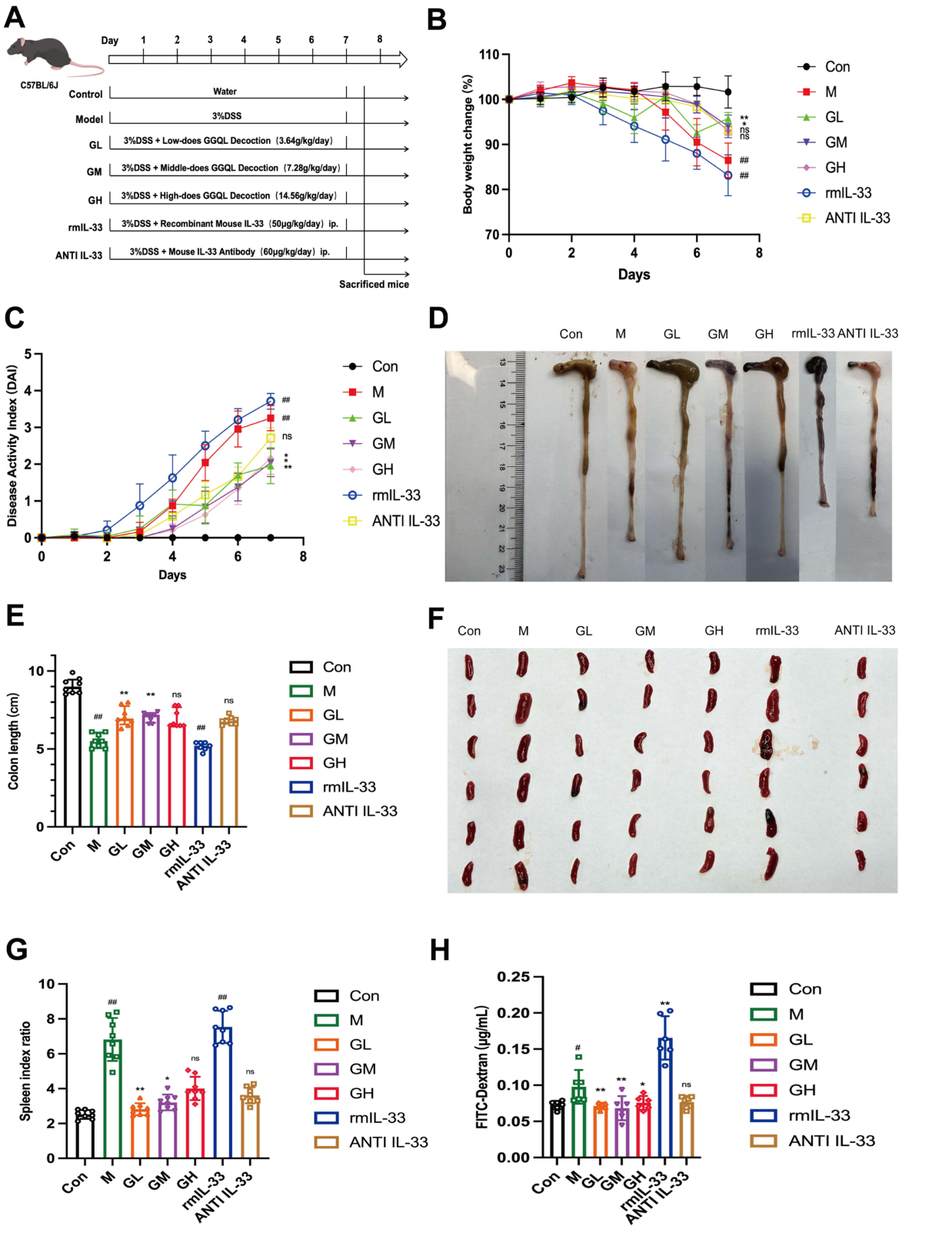

Figure 1 The protective effect of GGQLD against DSS-induced acute murine colitis is demonstrated. (**A**) Design diagram. (**B**) Weight change (n=8). (**C**) DAI scores (n=8). (**D**) Representative images of colons from each group. (**E**) Colon length (n=7-8). (**F**) Representative images of spleens. (**G**) Spleen weight index (n=8). (**H**) Serum concentration of FITC-dextran (n=6). (**I**) Representative colon histology (H&E staining, Minimum magnification 40X, maximum magnification 200X). (**J**) Histopathological scores of colon tissues (n=6). Values are mean ± SD. # $p < 0.05$, ## $p < 0.01$ versus Control; * $p < 0.05$, ** $p < 0.01$ versus DSS model; ns, not significant.

https://doi.org/10.2147/JIR.S601288

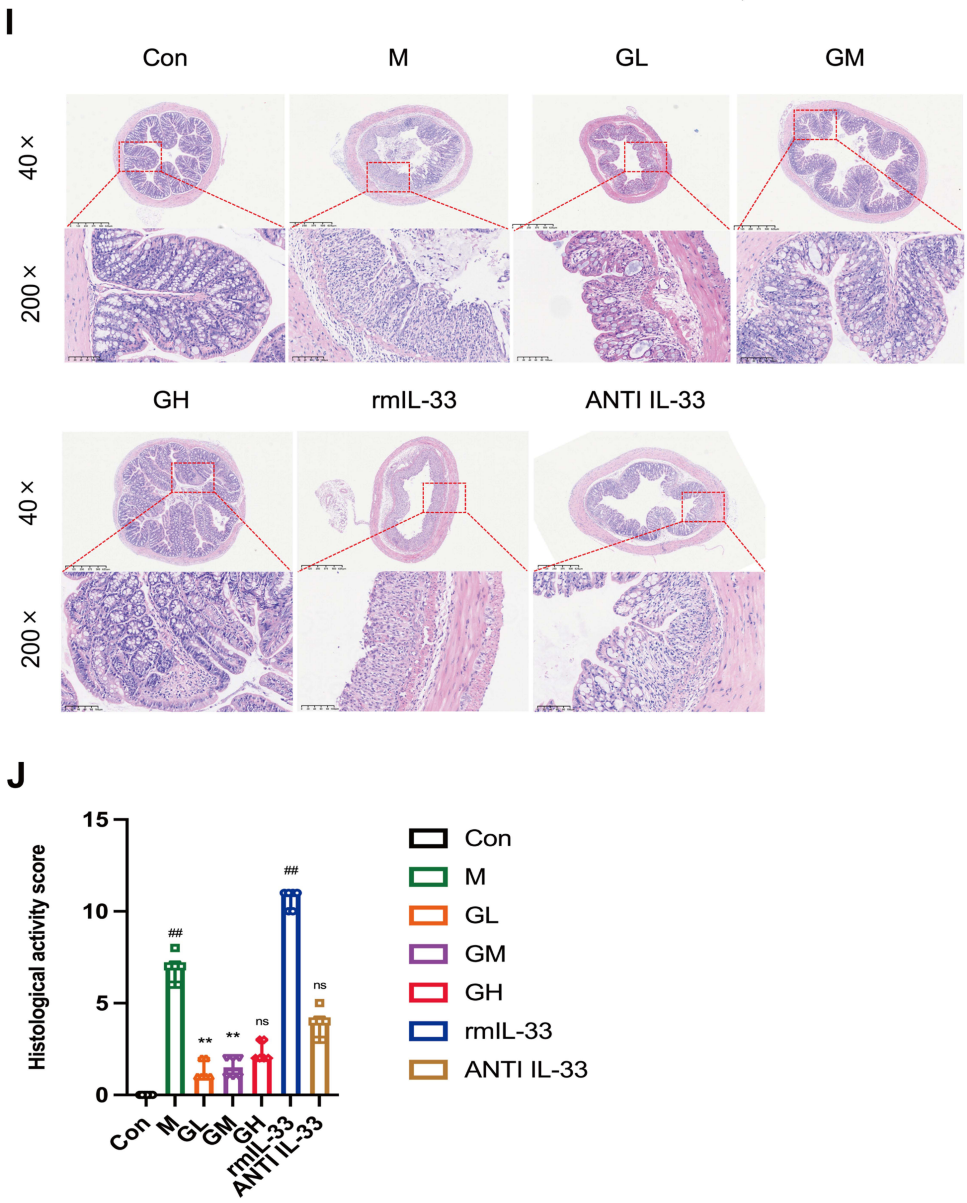

Figure 1 continued.

mounted for staining. The sections underwent H&E staining for histological examination. Histopathological scoring was performed according to established criteria (Table 2), with each parameter scored independently. A composite score was generated by summing the three subscores, resulting in a maximum possible score of 11.[44]

Table 1 Criteria for DAI Scoring in Mice

Weight Loss (%)	Fecal Consistency	Fecal Bleeding	Score
0	Normal	Normal (-)	0
1-5	Loose	Occult blood positive (+)	1
5-10	Soft	Slight gross blood (++)	2
10-15	Diarrhea	Gross blood (+++)	3
>15	Watery diarrhea	Severe gross blood (++++)	4

https://doi.org/10.2147/JIR.S601288

Table 2 Criteria for Histopathological Scoring of Colitis in Mice

Inflammatory Cell Infiltration	Crypt Damage	Ulceration	Score
Rare inflammatory cells in lamina propria	Intact crypts	No ulcer	0
Increased neutrophils in lamina propria	Loss of basal 1/3 crypts	1-2 ulcer foci	1
Inflammation extending into submucosa	Loss of basal 2/3 crypts	3-4 ulcer foci	2
Transmural inflammatory infiltration	Loss of entire crypts	Confluent or extensive ulcers	3
–	Epithelial surface erosion	–	4
–	Complete erosion of epithelial surface	–	5

Permeability of FITC-Dextran

The assessment of intestinal mucosal permeability was performed by measuring serum FITC-dextran (4 kDa; Sigma-Aldrich, Cat. No. 8004246) levels. Following a 4-hour fast on day 7, mice received an oral gavage of FITC-dextran (50 mg/kg in saline). Then we collected the blood 4 h later via the retro-orbital plexus. Samples were first centrifuged (3000 rpm, 15 min, 4°C) to obtain serum, which was protected from light prior to analysis. Fluorescence was recorded on a microplate reader with wavelengths set at 480 nm (excitation) and 520 nm (emission). Serum FITC-dextran concentration was determined from a standard curve.

Immunohistochemical (IHC) and Immunofluorescence (IF)

Colon sections (4 μm) were processed for IHC/IF. After standard processing (deparaffinization to antigen retrieval), overnight incubation with primary antibodies was carried out at 4°C. For IHC, antibodies included: anti-IL-33 (Proteintech, 12372-1-AP; 1:300), anti-ST2 (Abcam, ab228543; 1:200), anti-ZO-1 (Abcam, ab276131; 1:400), anti-E-cadherin (CST, 14472; 1:200), and anti-β-catenin (CST, 8480; 1:200). We performed DAB development on sections after secondary antibody incubation, followed by hematoxylin counterstaining and bright-field imaging. For IF, sections were probed with a combination of anti-IL-33 (Proteintech; 1:100) and anti-ST2 (Proteintech, 60112-1-lg; 1:50) primary antibodies. Sections were incubated with secondary antibodies (Alexa Fluor 488 anti-rabbit, 555 anti-mouse; 2 h, room temperature, dark), then nuclei were stained with Hoechst 33342. Finally, they were mounted with Beyotime anti-fade medium and visualized using a Zeiss LSM 800 confocal microscope. These assays were conducted to qualitatively evaluate protein localization and distribution. For each target, a minimum of three sections per animal and at least three animals in each group were analyzed, and representative images are presented in the figures.

Enzyme-Linked Immunosorbent Assay (ELISA)

Cytokine concentrations, including TNF-α, IL-4, and IL-10, in colon homogenates were quantified by ELISA kits following the manufacturer's protocols.

Flow Cytometry

We prepared a single-cell suspension from the colonic lamina propria. Briefly, a 30 mg segment of distal colon was opened longitudinally, washed in a solution containing D-PBS, FBS, HEPES, and EDTA at 37°C with shaking (200 rpm, 20 min). A single-cell suspension was prepared by digesting colon tissue. The tissue was subjected to enzymatic digestion at 37°C for 20 min with agitation (300 rpm) in FBS-supplemented RPMI-1640 medium, collagenase IV, Dispase, and DNase I, using a dedicated tissue dissociator. After filtration and washing, cell viability was assessed with Zombie Nir^{tm} Dye (APC-Cy7, 15 min, room temperature), followed by Fc receptor blockade using anti-CD16/32. For immunophenotyping, cells were incubated for 45 min at 4°C under light-protected conditions with a fluorescent antibody cocktail targeting CD45-FITC, CD11b-PerCP, F4/80-PE-Cy7, CD86-APC, and CD163-PE. For flow cytometry analysis, a sequential gating strategy was adopted. After excluding doublets using FSC-A/FSC-H and removing debris via forward/side scatter, viable cells were selected as Zombie NIR^{TM}-negative. Within the viable cell population, CD45^{+} leukocytes were gated, and then CD11b^{+}F4/80^{+} macrophages were identified. M1-and M2-like subsets were

distinguished based on CD86 and CD163 expression, respectively. Fluorescence-minus-one (FMO) controls served as gate references. Flow cytometry data acquisition was followed by analysis with FlowJo software.

Real-Time Quantitative PCR Amplification and Detection (qRT-PCR)

Total RNA from colon tissue was extracted using an RNApure Kit (CWBIO, China). RNA purity was assessed by NanoDrop One (Thermo Fisher Scientific); samples with A260/A280 ratios of 1.8–2.0 were used. Total RNA was reverse-transcribed using FastKing RT SuperMix (Tiangen). qPCR was run on a QuantStudio™ 5 system using SYBR Green PreMix (Tiangen). Thermal cycling: 95 °C for 15 min, then 40 cycles of 95 °C for 10s and 60 °C for 30 (fluorescence acquired at 60 °C). Melting curve analysis confirmed specificity. Relative expression ($2^{-\Delta\Delta Ct}$ method, normalized to Gapdh) was calculated with primers from Table 3.

Western Blot

Colon tissues were weighed and homogenized (1:10, w/v) in ice-cold RIPA buffer with protease and phosphatase inhibitors (2% each). Samples were processed using a chilled tissue grinder (60 Hz, 3×1 min, 10s intervals), followed by sonication on ice (100 Hz, 5 min), then centrifuged at 12,000 rpm for 15 min at 4 °C to collect supernatant. Protein levels were measured by BCA assay at 562 nm. Equal protein amounts (30 μg) were separated on 4–20% SDS-PAGE (80 V, 30 min; 110 V, 60 min) and transferred to 0.45 μm PVDF membranes using Servicebio transfer buffer (G2028, 400 mA, 30 min). After blocking with 5% milk in TBST (2 h, room temperature), primary antibodies (4°C, overnight) targeted: IL-33 (abcam ab187060; 1:1000), ST2 (abcam ab228543; 1:1000), Occludin (abcam ab216327; 1:1000), β-catenin (CST 8480; 1:1000), and E-cadherin (CST 14472; 1:1000). Membranes were then probed with HRP-secondary antibodies (CST; 1:5000) for 2 h. Signals were detected using ECL substrate and imaged with a Bio-Rad ChemiDoc™ system. Band intensities were quantified using ImageJ and normalized to β-actin (Proteintech 66009-1-lg; 1:20,000).

Data Analysis

All statistical analyses were performed using SPSS 26.0, and data are presented as mean ± standard deviation (SD). Normality was assessed using the Shapiro–Wilk test, and homogeneity of variance was evaluated using Levene's test. Differences among multiple groups were analyzed by one-way ANOVA followed by Tukey's HSD post hoc test when appropriate. Comparisons between two groups were performed using an unpaired two-tailed Student's *t*-test. When assumptions of normality or equal variance were not met, the Kruskal–Wallis test with Bonferroni correction was applied.

Samples were excluded only when predefined quality-control criteria were not met, including incomplete tissue specimens that precluded reliable measurement, sample loss during preparation, or technical assay errors. Details regarding excluded samples and the corresponding reasons are provided in Supplementary Table S1 (Supplementary

Table 3 Mouse Gene Primer Sequences

Gene	Primer Sequences (5' to 3')
mGAPDH F	CTTCAACAGCAACTCCCACTCTTCC
mGAPDH R	GGTGGTCCAGGGTTTCTTACTCC
mIL-33 F	GCGGAATCTGCGTCATTCCT
mIL-33 R	TTGTGGTCACACGTGGTTTT
mST2 F	GCAATTCTGACACTTCCCATG
mST2 R	ACGATTTACTGCCCTCCGTA
mZO-1 F	TCTTGCAAAGTATCCCTTCTGT
mZO-1 R	CAGAAATCGTGCTGATGTGCC
mβ-catenin F	CCCAGTCCTTCACGCAAGAG
mβ-catenin R	CATCTAGCGTCTCAGGGAACA
mOccludin F	ATGCGGAAAGAGTCGACAGTCCAA
mOccludin R	AAGTCATCCACGGACAAGGTCAGA

Materials 1). Sample sizes (n) are indicated in the respective figure legends. Original Western blot images are provided in the Supplementary Materials (Supplementary Materials 2). Statistical significance was defined as $p < 0.05$ ($*p < 0.05$, $**p < 0.01$). Graphical representations were prepared using GraphPad Prism 10.

Results

Analysis of Signature Constituents in Gegen Qinlian Decoction

UPLC-MS-based chemical profiling was conducted to establish the quantitative attributes of eight predominant compounds present in Gegen Qinlian Decoction. The specific concentrations derived for these eight analytes are detailed in Table 4.

Effects of GGQLD and IL-33-Targeted Interventions on DSS-Induced Acute Colitis

Compared with control group, DSS-treated C57BL/6J mice showed a significant decrease in body weight (Figure 1B), elevated DAI scores (Figure 1C), marked colon shortening (Figure 1D and E), and an increased spleen weight index (Figure 1F and G), indicating the successful induction of acute colitis following a 7-day administration of 3% DSS in drinking water. H&E staining of colon tissue further revealed severe pathological changes in the model group, including intense inflammatory infiltration, crypt destruction, epithelial damage, and ulcer formation (Figure 1I and J). Consistent with barrier dysfunction, intestinal permeability assessed by FITC-dextran assay was markedly elevated in DSS mice relative to controls (Figure 1H). These observed phenotypic and pathological changes are indicative of successful establishment of an acute DSS-induced colitis model.

Treatment with GGQLD at various doses ameliorated these pathological features to different extents. Notably, the low-dose (GL) and medium-dose (GM) GGQLD groups showed significant improvements, attenuating body weight loss (Figure 1B), reducing DAI scores (Figure 1C), alleviating colon shortening (Figure 1D and E), and suppressing spleen enlargement (Figure 1F and G). Histopathological scoring indicated that GL and GM treatment significantly mitigated inflammatory damage and better preserved crypt architecture (Figure 1I and J). The marked decrease in serum FITC-dextran across all GGQLD groups (Figure 1H) is consistent with a protective role of the treatment in DSS colitis.

Following intervention in IL-33 signaling, sustained rmIL-33 administration aggravated colitis pathology. Compared with the DSS model group, the IL-33 group exhibited more pronounced splenomegaly (Figure 1F and G) and further increased intestinal permeability (Figure 1H), suggesting enhanced systemic immune activation and barrier disruption. In contrast, treatment with an IL-33-neutralizing antibody (ANTI IL-33 group) produced protective effects similar to those observed with GGQLD, including significant reduction of the spleen weight index (Figure 1F and G) and improvement of other colitis-related phenotypes. Collectively, these findings suggest that suppression of IL-33 signaling may contribute, at least in part, to the therapeutic effects of GGQLD.

Table 4 Contents of Eight Major Compounds in Gegen Qinlian Decoction

Name	Retention Time (min)	Content (mg/g)
Puerarin	2.82	93.17
Daidzin	3.67	26.18
Baicalin	6.77	41.39
Wogonoside	8.42	18.59
Palmatine	7.33	18.50
Berberine	7.39	35.88
Liquiritin	4.56	2.75
Glycyrrhizic acid	13.61	10.61

https://doi.org/10.2147/JIR.S601288

GGQLD Ameliorates DSS-Induced Colitis and is Associated with Modulation of the IL-33/ST2 Pathway

To explore whether GGQLD acts in association with the IL-33/ST2 pathway, we first examined the expression and localization of key molecules in colon tissue. Qualitative assessment by IHC showed that in control mice, IL-33 was primarily localized to colonic mucosal epithelial cells (Figure 2A), while its receptor ST2 was only weakly observed in the epithelial layer and lamina propria (Figure 2B). Altered expression patterns of IL-33 and ST2 were observed in colon tissues from the DSS model and rmIL-33 groups. Specifically, IL-33 immunoreactivity was notably enhanced within inflammatory infiltrates and residual epithelial cells, whereas it appeared diffusely weak in areas where the glandular architecture was destroyed (Figure 2A). ST2 showed diffuse expression in damaged glandular areas and abnormally high expression in some residual glandular regions (Figure 2B). Treatment with GGQLD or the anti-IL-33 antibody was associated with a more regular distribution pattern of IL-33 and less extensive ST2 staining in damaged areas (Figure 2A and B).

IF analysis revealed similar spatial distribution patterns. In control tissue, IL-33 signal was predominantly localized to the intestinal epithelium, whereas ST2 staining was weak and sparsely distributed. The DSS model group showed partial co-localization of IL-33 and ST2. In the rmIL-33 group, severe epithelial disruption was associated with a reduction in IL-33 signal but an abnormal accumulation of ST2 signal in inflamed areas. After the treatment of GGQLD or anti-IL-33 antibody, the fluorescence intensity and distribution range of ST2 in the lamina propria were reduced compared to the model group (Figure 2C). These observations suggest that DSS-induced colitis disrupts the physiological distribution pattern of the IL-33/ST2 axis, leading to aberrant overexpression and co-localization in inflamed and damaged regions. GGQLD and the anti-IL-33 antibody were associated with a more localized distribution of IL-33 and reduced ST2 signal dispersion in damaged regions, accompanied by partial restoration of the spatial expression pattern of this pathway. To quantitatively evaluate these observations, IL-33 and ST2 expression were further assessed by qPCR and Western blotting. Relative to the control, both the DSS model and rmIL-33 groups showed significant upregulation in the gene expression of IL-33 and ST2, along with increased ST2 protein expression (Figure 2D, E and G). IL-33 protein was significantly elevated in the model group versus controls, while levels in the rmIL-33 group showed no statistical change (Figure 2F). Following treatment, all GGQLD groups exhibited varying degrees of reduction in IL-33 mRNA and protein expression levels (Figure 2D, F). A decrease in ST2 mRNA expression was observed in the high-dose GGQLD group (Figure 2E), whereas lower ST2 protein expression was detected in the low-dose GGQLD group (Figure 2G). Collectively, these findings indicate that GGQLD treatment was accompanied by alterations in IL-33/ST2 pathway-related molecules at both the transcriptional and translational levels.

Effects of GGQLD and IL-33 Intervention on Macrophage Phenotypes and Inflammatory Cytokines

A significant reduction in the M2-like/M1-like macrophage ratio was observed in the splenic tissue of DSS model group relative to the control, as revealed by flow cytometry (Figure 3A, B and E). This ratio was further reduced in the rmIL-33 group but was markedly increased in GGQLD-treated groups. In colon tissue, the frequency of $CD163^{+}$ M2-like macrophages showed significant variation across groups. Relative to controls, it was reduced in the model group, showed a more pronounced reduction with rmIL-33 treatment, and was restored in mice receiving GGQLD (Figure 3C, D). ELISA analysis of colon tissues showed an inverse pattern in cytokine levels: pro-inflammatory TNF-α was significantly increased (Figure 3G), while anti-inflammatory IL-4 and IL-10 were decreased in the DSS model and rmIL-33 groups compared to controls (Figure 3F, H). Compared to the model group, low- and medium-dose GGQLD treatment reduced TNF-α expression (Figure 3G). All GGQLD treatment groups increased IL-4 levels to varying degrees, with the low-dose group showing a significant elevation in IL-10 content (Figure 3F and H). These results indicate that GGQLD treatment was associated with effective alleviation of acute intestinal inflammatory injury induced by DSS.

Taken together, these findings suggest that exogenous IL-33 is associated with exacerbated colitis, enhanced M1-like responses, and a pro-inflammatory state. Conversely, GGQLD treatment was accompanied by reduced IL-33/ST2 signaling, a shift toward M2-like macrophage features, and alleviation of colonic inflammation.

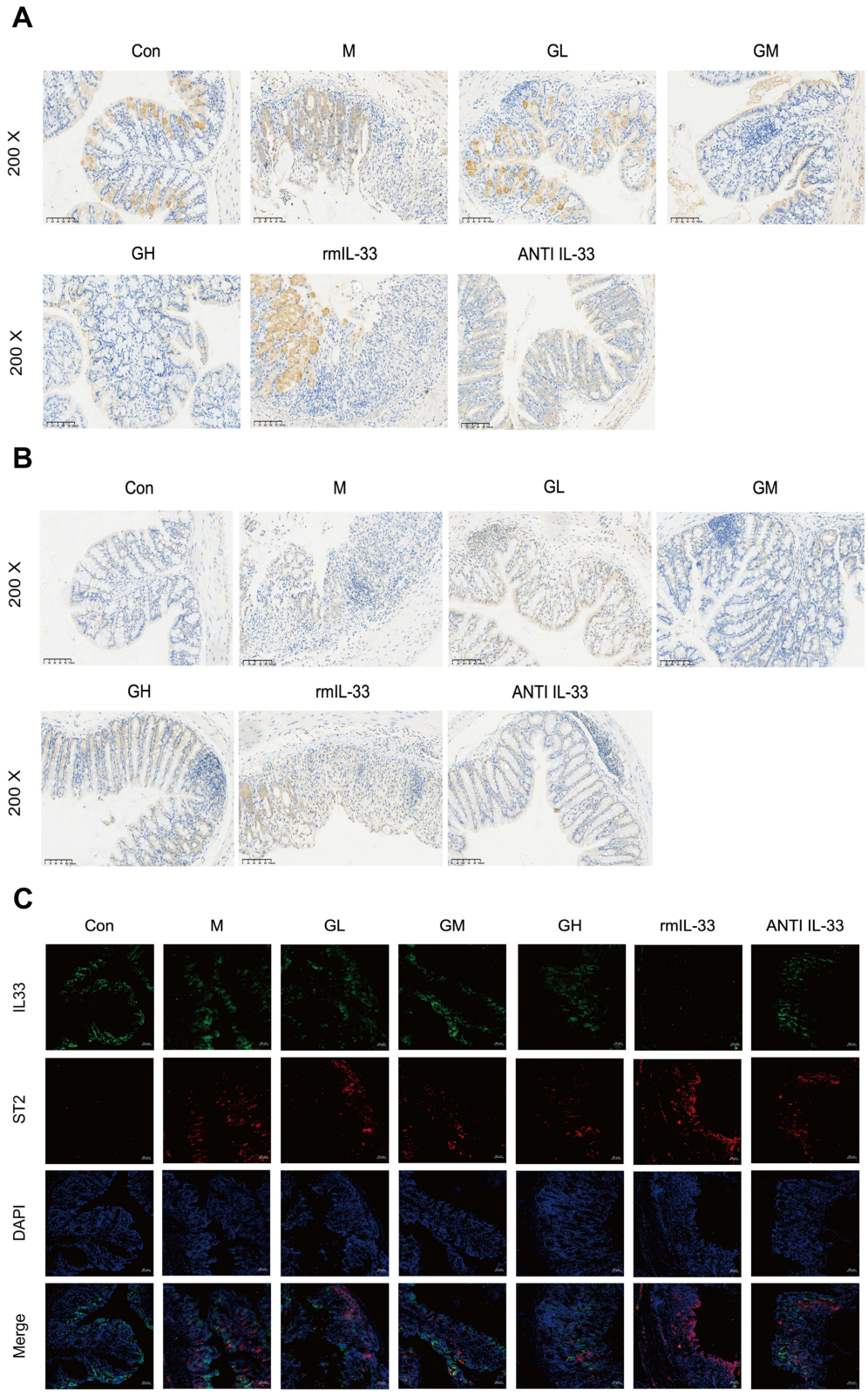

Figure 2 GGQLD alleviates DSS-induced colitis with reduced IL-33/ST2 signaling activity. (**A**) IL-33 immunostaining (colon). (**B**) ST2 immunostaining (colon). (**C**) Representative immunofluorescence images showing the localization of IL-33 (green) and ST2 (red) in colon tissues (100X). Nuclei were counterstained with DAPI (blue). (**D**) Levels of IL-33 mRNA (n=6). (**E**) Levels of ST2 mRNA (n=6). (**F**) IL-33 protein levels were detected by Western blot (n=5). (**G**) ST2 protein levels were detected by Western blot (n=5). Values are mean ± SD. # $p < 0.05$, ## $p < 0.01$ versus Control; * $p < 0.05$, ** $p < 0.01$ versus DSS model; ns, not significant.

https://doi.org/10.2147/JIR.S601288

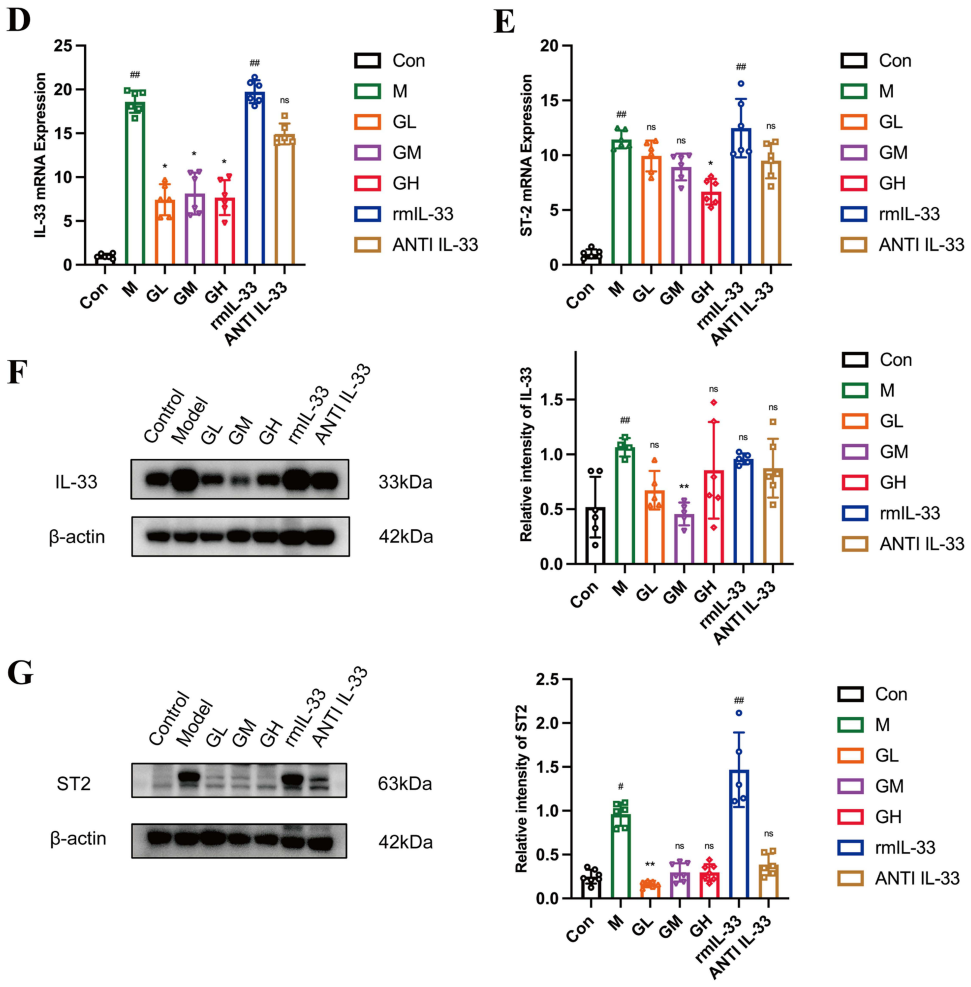

Figure 2 continued.

Effects of GGQLD and IL-33 Intervention on Intestinal Barrier Function

To evaluate the potential effects of GGQLD on intestinal epithelial barrier integrity, we first examined the localization and staining patterns of key barrier proteins by IHC. In control mice, the tight junction protein ZO-1 displayed a continuous linear staining pattern between adjacent epithelial cells (Figure 4A). Similarly, the adherens junction proteins β-catenin and E-cadherin exhibited continuous and well-organized staining along the epithelial layer (Figure 4B and C). In the DSS model and rmIL-33 groups, the staining patterns and spatial distribution of these barrier proteins were markedly disrupted. ZO-1 staining appeared fragmented and discontinuous (Figure 4A); β-catenin staining was reduced or absent in damaged glandular regions and disorganized in the remaining epithelium (Figure 4B); and E-cadherin exhibited irregular staining in inflamed areas with loss of continuity in severely damaged glands (Figure 4C). Treatment with GGQLD or anti-IL-33 antibody was associated with partial restoration of barrier protein distribution and staining continuity. Specifically, ZO-1 exhibited a more continuous linear staining pattern within crypt and glandular regions (Figure 4A), β-catenin staining appeared more organized in glandular areas (Figure 4B), and E-cadherin showed improved staining continuity in epithelial regions (Figure 4C).

To complement the qualitative histological observations described above, qPCR and Western blot analyses were performed to quantitatively evaluate the expression of barrier-related genes and proteins. Compared with the control group, both the DSS and rmIL-33 groups exhibited significantly reduced mRNA expression of Occludin, β-catenin, and ZO-1 (Figure 4D–F). At the protein level, Occludin expression was decreased in both groups (Figure 4G). In addition, β-

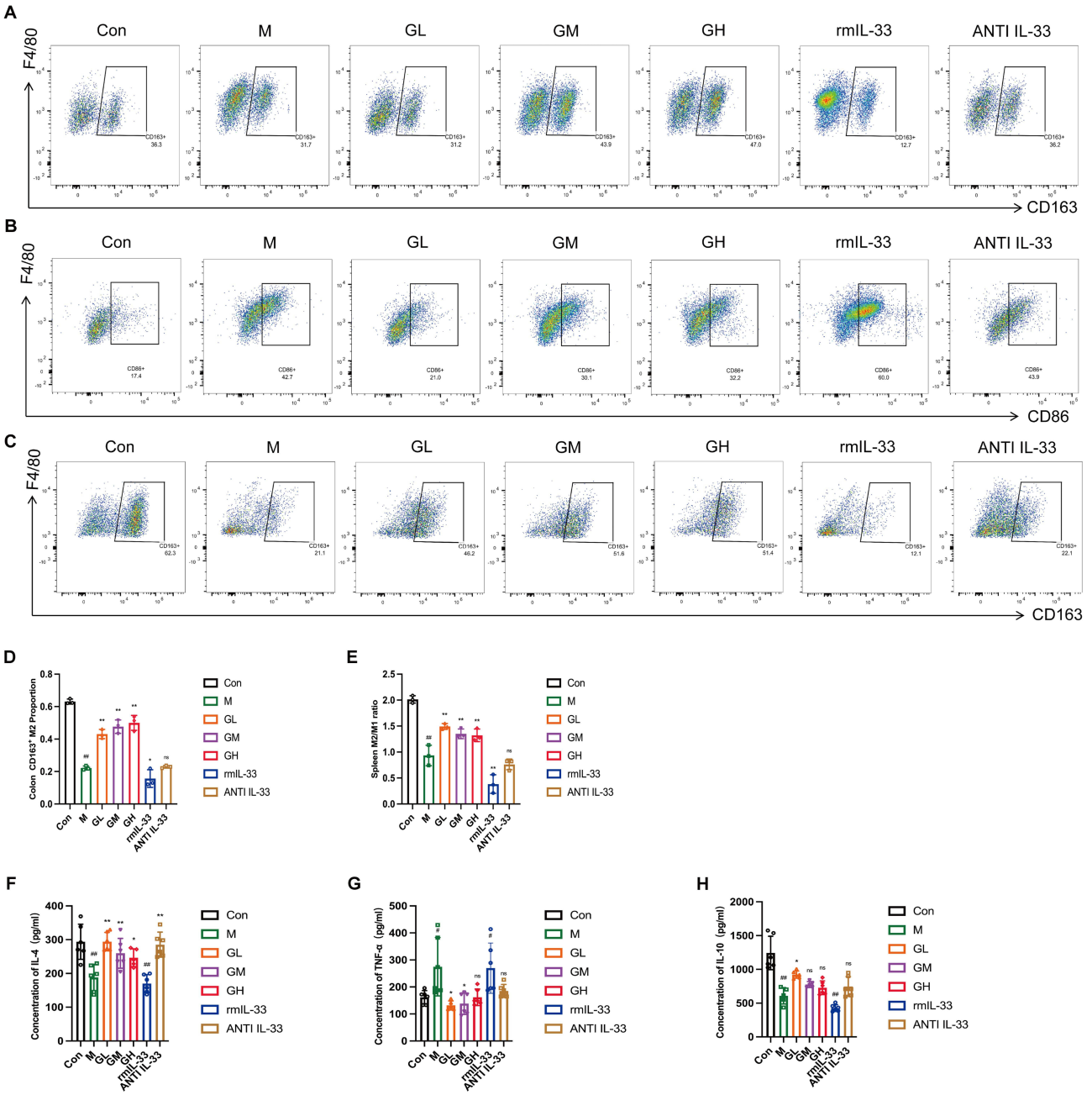

Figure 3 Effects of GGQLD and IL-33 intervention on macrophage phenotypes and inflammatory cytokines. (**A**) Gating strategy for splenic M2-like macrophages ($CD163^+$) (**B**) Gating strategy for splenic M1-like macrophages ($CD86^+$) (**C**) Gating strategy for colonic M2-like macrophages ($CD163^+$). (**D**) Percentage of CD163+ M2-like macrophages in the colon (n=3). (**E**) Ratio of CD163+ M2-like to CD86+ M1-like macrophage percentages in the spleen (n=3). (**F**) Quantification of colonic IL-4 protein by ELISA (n=5-6). (**G**) Quantification of colonic TNF-α protein by ELISA (n=5-6).. (**H**) Quantification of colonic IL-10 protein by ELISA (n=5-6). Values are mean ± SD. # $p < 0.05$, ## $p < 0.01$ versus Control; * $p < 0.05$, ** $p < 0.01$ versus DSS model; ns, not significant.

catenin protein expression was reduced in the DSS group, whereas E-cadherin protein expression was decreased in the rmIL-33 group (Figure 4H–I). Following pharmacological intervention, GGQLD treatment was associated with varying degrees of recovery in the mRNA and protein expression of key barrier molecules, including Occludin, β-catenin, ZO-1, and E-cadherin (Figure 4D–I). Moreover, administration of the anti-IL-33 antibody significantly increased β-catenin protein levels (Figure 4H).

Both DSS challenge and exogenous IL-33 disrupted the expression and localization of key epithelial barrier proteins. In contrast, GGQLD improved mucosal barrier integrity in colitis mice, together with reduced IL-33 signaling activity.

https://doi.org/10.2147/JIR.S601288

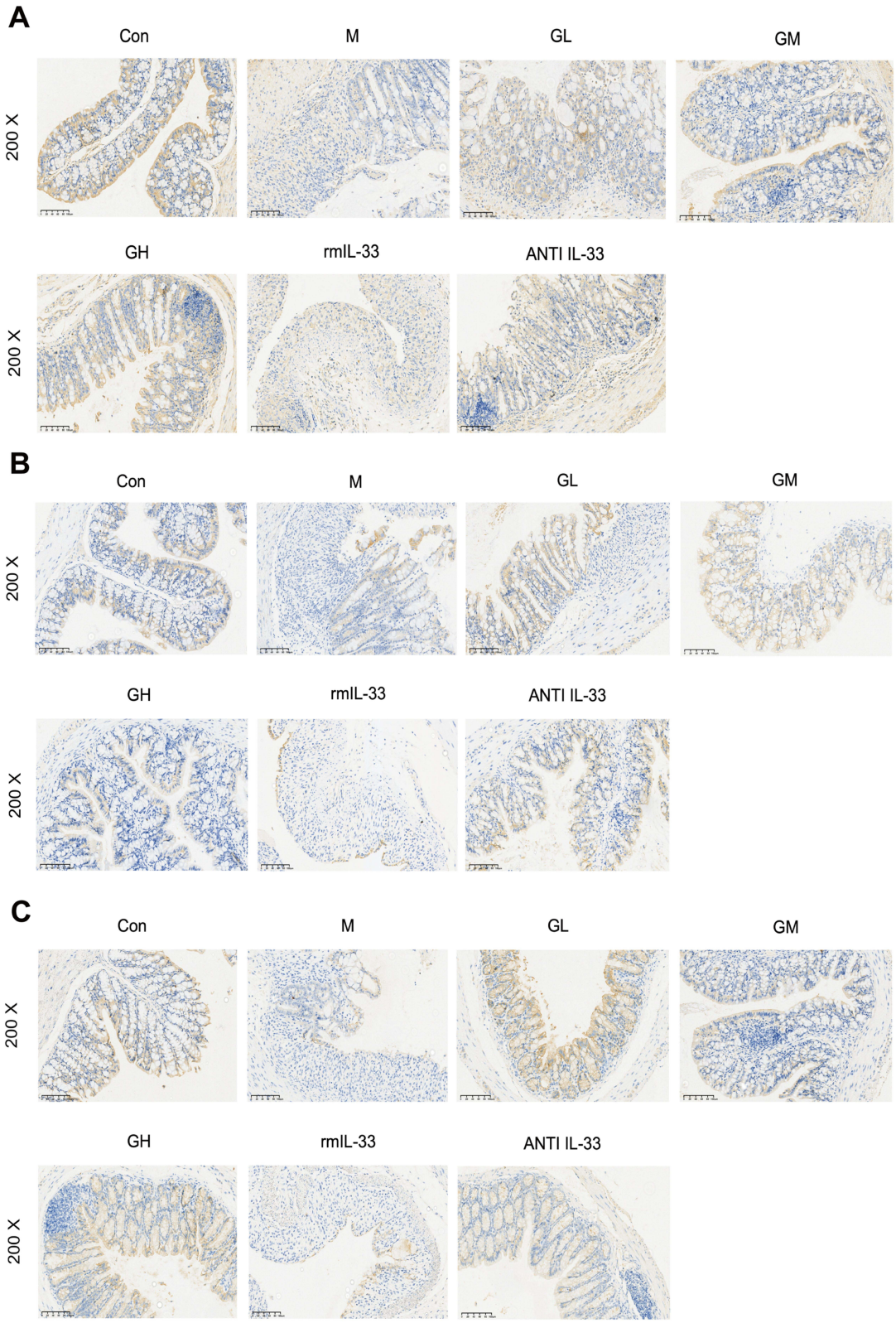

Figure 4 GGQLD improves gut mucosal barrier dysfunction in mice with acute colitis. (**A**) ZO-1 immunostaining (colon). (**B**) β-catenin immunostaining (colon). (**C**) E-cadherin immunostaining (colon). (**D**) Levels of ZO-1 mRNA (n=6). (**E**) Levels of Occludin mRNA (n=6). (**F**) Levels of β-catenin mRNA (n=6). (**G**) Representative immunoblots of Occludin (n=5). (**H**) Representative immunoblots of β-catenin (n=5). (**I**) Representative immunoblots of E-cadherin (n=5). Values are mean ± SD. # $p < 0.05$, ## $p < 0.01$ versus Control; * $p < 0.05$, ** $p < 0.01$ versus DSS model; ns, not significant.

https://doi.org/10.2147/JIR.S601288

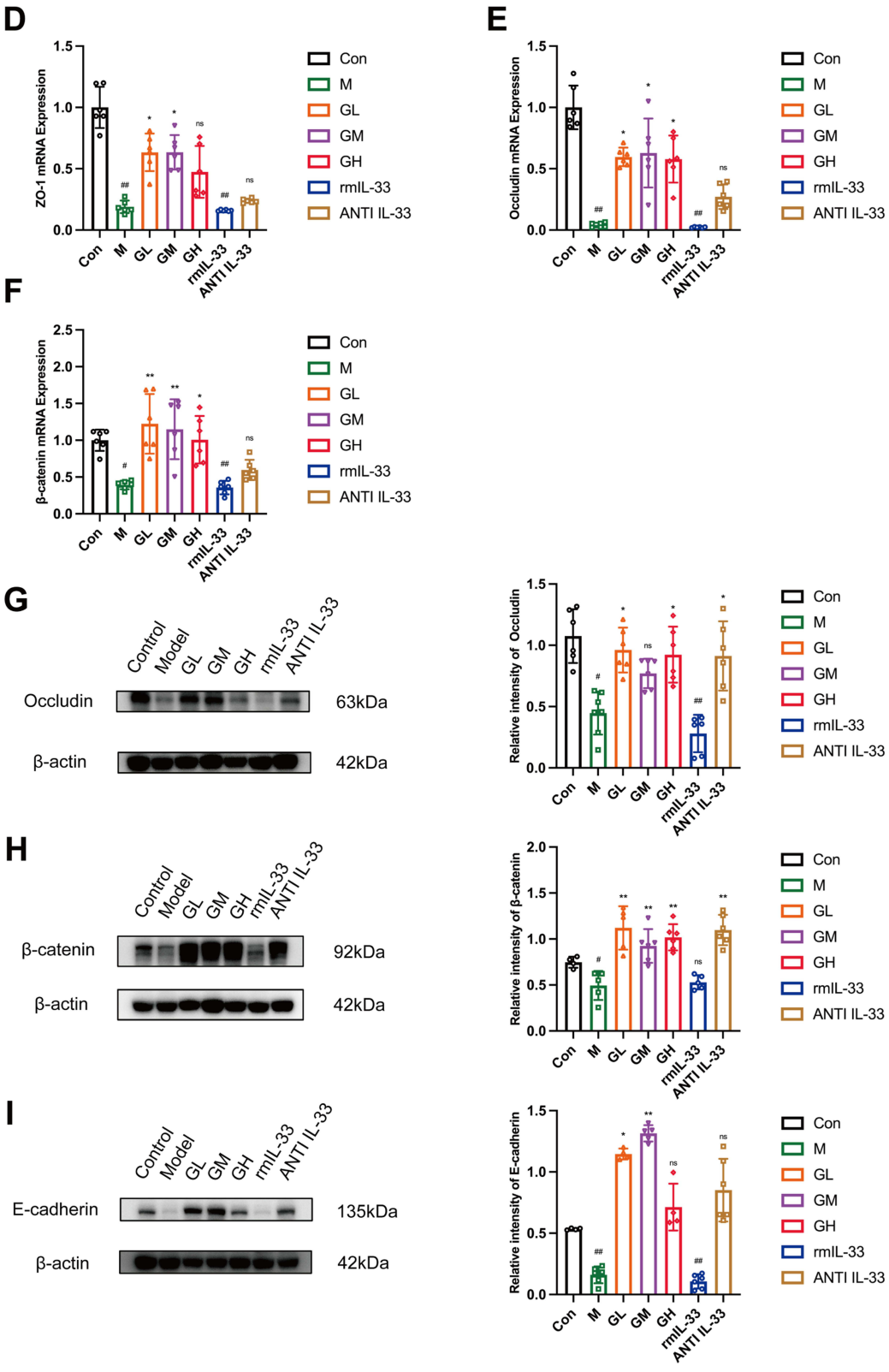

Figure 4 continued.

https://doi.org/10.2147/JIR.S601288

Discussion

The pathogenesis of UC, a major inflammatory bowel disease (IBD), involves a multifactorial etiology where genetic susceptibility, immune dysregulation, environmental triggers, and impaired intestinal barrier function are involved. In recent years, targeting immune modulation has become a pivotal therapeutic strategy for UC. Of particular note, the potential association between the IL-33/ST2 signaling pathway and macrophage phenotypic regulation has attracted increasing attention. For instance, TsSPIs from Trichinella spiralis were shown to alleviate TNBS-colitis via IL-33/ST2 axis downregulation and M2-like phenotype.[45] Their work provided preliminary evidence supporting the therapeutic relevance of targeting both the IL-33/ST2 pathway and macrophage phenotypic regulation in IBD. Against this background, we report here the novel finding that GGQLD protects against experimental acute colitis induced by DSS, and these protective effects are associated with suppression of the IL-33/ST2 signaling axis and increased proportions of $CD163^+$ M2-like macrophages. Our findings align with previous observations regarding the IL-33/ST2-macrophage interaction and further suggest that GGQLD treatment was accompanied by restoration of key intestinal epithelial junctional proteins, including tight junction components (ZO-1, Occludin) and adherens junction proteins (E-cadherin, β-catenin).

Collectively, these results support a potential association between GGQLD treatment and modulation of the IL-33/ST2 axis, although definitive causal relationships remain to be established. To evaluate these findings, a multi-parametric approach was used.[46] DAI score, changes in body weight, colon length, and spleen index were employed as parameters to evaluate disease severity and systemic immune activation.[47–50] Histopathological scoring further allowed for quantitative microscopic evaluation of mucosal architecture and inflammatory damage. Complementing these macroscopic and histological measures, the FITC-dextran permeability assay offered a functional readout of intestinal barrier integrity, while IHC and IF analyses provided spatial context for molecular changes. Together, these complementary methods help to strengthen the overall evidence supporting the protective effects of GGQLD observed in this model.

IL-33/ST2 signaling exhibits context-dependent functional duality in gut immunity.[17,51–54] It has been reported to promote type 2 responses, enhance IL-13 production, and be associated with M2-like phenotype and tissue repair.[55–60] Conversely, it may also amplify TNF-α- and IFN-γ-mediated type 1 responses under certain inflammatory conditions, contributing to tissue injury.[61–68] Our findings are consistent with this context-dependent behavior and should therefore be interpreted within the specific setting of acute DSS-induced colitis rather than as a broadly generalizable mechanism.

For example, intermittent rmIL-33 (days 0, 2, 5) ameliorated DSS colitis,[42] whereas our continuous daily rmIL-33 for 7 days aggravated colitis—likely reflecting over-activation of inflammatory pathways under sustained exposure. These contrasting observations further illustrate the highly context-sensitive nature of IL-33/ST2 signaling and caution against extrapolating acute model findings to chronic, relapsing disease.

Evidence from clinical investigations indicates that the levels of IL-33 and ST2 are significantly increased in the colonic mucosa of UC patients during inflammation.[53,69–71] Functional studies further suggest a pathogenic contribution of this axis, as genetic deficiency of IL-33 or ST2 confers increased resistance to DSS-induced colitis and delays the onset of inflammatory responses.[72,73] Notably, Sedhom et al reported that ST2 deficiency preserved the expression of connexin 43—a gap junction protein essential for epithelial migration and repair—which was associated with improved mucosal healing following injury.[18] Collectively, these findings suggest that excessive activation of IL-33/ST2 signaling may contribute to impaired epithelial restitution.

At the molecular level, IL-33 has been shown to regulate multiple proteins critical for epithelial integrity, including E-cadherin, ZO-1, and Occludin.[74,75] Consistent with these observations, our results demonstrated that exogenous IL-33 administration in DSS-treated mice further reduced the expression and disrupted the spatial distribution of β-catenin and E-cadherin. These findings are consistent with the possibility that, within an inflammatory microenvironment, sustained activation of the IL-33/ST2 axis may compromise epithelial barrier structure and function. Mechanistically, IL-33 binding to ST2 can activate the protein kinase A (PKA) pathway, which has been reported to be associated with phosphorylation of β-catenin at Ser675/Ser552, as well as changes in β-catenin stability, nuclear localization, and barrier-associated protein expression such as E-cadherin.[76,77] GGQLD treatment was associated with restoration of both mRNA and protein levels of these junctional components, together with improved continuity of their tissue distribution.

A similar trend was observed following IL-33 neutralization. These observations suggest that GGQLD may contribute to improvement of the epithelial barrier through coordinated regulation of IL-33 activity and the inflammatory microenvironment, rather than acting via a single defined pathway.

Macrophages are critical innate immune cells that participate in early mucosal defense and inflammatory regulation.[78] Owing to their remarkable plasticity, macrophages can adopt distinct functional phenotypes in response to environmental cues.[79] Under pro-inflammatory conditions, they polarize toward an M1 phenotype characterized by the production of TNF-α and IFN-γ, thereby amplifying tissue damage.[80] In contrast, anti-inflammatory signals promote M2-like phenotype, which is associated with the secretion of mediators such as Arg1, YM-1, and IL-10, contributing to tissue repair and resolution of inflammation.[81,82]

CD163 serves not only as a canonical surface marker of M2-like macrophages,[80] but also as a scavenger receptor capable of directly inducing IL-10 production upon activation.[83,84] An imbalance in macrophage polarization, typically reflected by an elevated M1-like/M2-like ratio, has been observed in both systemic circulation and colonic tissues of UC patients,[25,26] highlighting the M1-like/M2-like equilibrium as a potential therapeutic target.[26,27]

The IL-33/ST2 axis has been implicated in the regulation of immune responses and may be associated with macrophage phenotypic changes.[85] Mechanistic studies indicate that IL-33/ST2 signaling can influence macrophage phenotypic regulation through multiple pathways, although the direction of this effect appears to be highly dependent on the inflammatory context. For instance, activation of the PI3K/AKT/mTOR pathway suppresses autophagy and favors M2 differentiation,[86] while MAPK signaling (ERK/JNK/p38) has also been implicated in this process.[87] These findings are broadly consistent with our observations that GGQLD treatment is associated with suppression of IL-33/ST2 signaling and an increased proportion of $CD163^+$ M2-like macrophages. Moreover, the changes observed following exogenous IL-33 administration further suggest a potential involvement of this pathway.

However, it should be noted that autophagy flux and MAPK activation were not directly assessed in the present study. Therefore, the downstream mechanisms underlying the association between IL-33/ST2 signaling and macrophage phenotypic changes in colitis remain to be elucidated. In addition, IL-33 may regulate macrophage function both indirectly—via induction of cytokines such as IL-13—and directly, potentially through modulation of mitochondrial metabolic reprogramming.[57,88] Emerging evidence indicates that IL-33 exerts bidirectional effects on macrophage phenotypic changes in a microenvironment-dependent manner. While it may promote an M2-like phenotype and tissue repair under certain conditions,[22] it may also enhance M1-associated responses in pro-inflammatory settings.[23] This functional plasticity may, in part, be mediated by metabolic reprogramming. For example, IL-33/ST2 signaling has been proposed to regulate the expression of PGC-1α, a key regulator of mitochondrial biogenesis and cellular energy metabolism.[89]

This context-dependent mechanism may help explain our observations that sustained IL-33 stimulation aggravated DSS-induced colitis and reduced the ratio of $CD163^+$ to $CD86^+$ splenic macrophages, whereas IL-33 neutralization reversed these effects. In parallel, GGQLD treatment was associated with increased $CD163^+$ M2-like macrophages and elevated IL-10 levels, along with reduced TNF-α expression. Taken together, these findings support the hypothesis that the therapeutic effects of GGQLD may be associated, at least in part, with modulation of the IL-33/ST2 axis, which was accompanied by a shift toward a repair-associated macrophage phenotype and features consistent with improved intestinal immune homeostasis.

Our study suggests a potential association among IL-33/ST2 signaling, macrophage phenotypic changes, and epithelial barrier repair in the context of GGQLD treatment. This observation is supported by combined gain- and loss-of-function approaches using recombinant IL-33 and neutralizing antibodies. However, several limitations should be acknowledged. First, the study did not include a combined intervention group receiving both GGQLD and exogenous IL-33. The absence of such a rescue experiment limits the ability to determine whether inhibition of IL-33 is a necessary condition for the therapeutic effects of GGQLD, thereby restricting causal inference. Second, the in vivo assessment of macrophage phenotype does not allow discrimination between direct pharmacological actions and indirect effects mediated by changes in the inflammatory microenvironment. Third, the downstream signaling mechanisms linking IL-33/ST2 activation to macrophage phenotypic changes in colitis were not directly examined and remain to be clarified. Fourth, although the acute DSS model reproduces key features of intestinal inflammation, it does not fully reflect the

chronic, relapsing-remitting nature of human UC. Future studies should validate these findings in chronic or more clinically relevant models, and incorporate advanced approaches such as lineage-specific conditional knockout of IL-33 or ST2 and single-cell transcriptomic analysis to better define the interactions between the bioactive components of GGQLD and their molecular targets, which may support future clinical translation. More broadly, the development of microenvironment-responsive drug delivery systems—such as ROS-responsive nanoparticles for targeted and multi-functional delivery in IBD—represents a promising direction for improving the precision of natural product-based therapies.[90] These strategies may help overcome inherent limitations of orally administered herbal formulations, including variable bioavailability and off-target systemic exposure.

In addition, given that GGQLD undergoes hepatic first-pass metabolism, it is plausible that its bioactive components may initially modulate hepatic signaling pathways, such as Nrf2 activation,[91,92] thereby reducing systemic oxidative stress and indirectly influencing intestinal inflammation. This potential liver-systemic-intestinal axis is not addressed in the present study and warrants further investigation.

Conclusion

In summary, the present study shows that administration of GGQLD alleviates disease severity in mice with DSS-induced acute colitis. This protective effect is associated with attenuation of IL-33/ST2 signaling, an increased proportion of $CD163^+$ M2-like macrophages, and improved epithelial barrier integrity. While the precise causal relationships among these observations remain to be fully established, the findings suggest that modulation of the IL-33/ST2 axis and macrophage phenotypic changes may contribute to the beneficial effects observed following GGQLD treatment. Collectively, these results provide a basis for further investigation into the therapeutic relevance of this signaling network and its potential as a target for immunomodulatory strategies in ulcerative colitis.

Abbreviations

GGQLD, Gegen Qinlian Decoction; UC, Ulcerative colitis; DSS, Dextran sulfate sodium; IL-33, Interleukin-33; ST2, Tumorigenicity 2; TCM, Traditional Chinese medicine; DAI, Disease activity index; H&E, Hematoxylin and eosin; IHC, Immunohistochemical; IF, Immunofluorescence; ELISA, Enzyme-linked immunosorbent assay; qRT-PCR, Quantitative Real-Time PCR; Treg, Regulatory T; IBD, Inflammatory bowel disease.

Data Sharing Statement

The original contributions presented in this study are included in the article. Further inquiries can be directed to the corresponding author.

Ethical Review and Participant Consent

All animal procedures conducted in this research received ethical approval from the Institutional Animal Care and Use Committee of Guangzhou University of Chinese Medicine. All animal experiments were performed in accordance with the Guide for the Care and Use of Laboratory Animals and institutional guidelines for animal welfare. This study is reported in compliance with the ARRIVE guidelines.

Author Contributions

Lin-Xu; Conceptualization, Funding acquisition, Writing-review and editing. Yuqi-Wu; Formal analysis, Investigation, Project administration, Writing-original draft. Mengqing-Ma; Data curation, Methodology, Funding acquisition, Writing-original draft. Liuru-Luo Investigation, Validation, Writing-review and editing. Weijian-Zhang; Visualization, Writing-review and editing. Xinxin-Hong; Formal analysis, Writing-review and editing. Xiaoyan-Jiang; Funding acquisition, Project administration, Writing-review and editing. Junyi-Li; Software, Writing-review and editing. Sihui-Zeng; Validation, Writing-review and editing. Kexin-Li; Investigation, Writing-review and editing. Huishan-Yuan; Formal analysis, Writing-review and editing. Shaoju-Guo; Resource, Writing-review and editing. All authors gave final approval of the version to be published; have agreed on the journal to which the article has been submitted; and agree to be accountable for all aspects of the work.

Funding

This study was supported by the National Natural Science Foundation of China (82204994), China postdoctoral science foundation (2025M773958), Shenzhen Science and Technology Program (JCYJ20230807094459047), Traditional Chinese Medicine Bureau of Guangdong Province Program (20241269), Sanming Project of Medicine in Shenzhen (SZZYSM202211002).

Disclosure

The authors declare that they have no known competing financial interests or personal relationships that could have appeared to influence the work reported in this paper.

References

1. Le Berre C, Honap S, Peyrin-Biroulet L. Ulcerative colitis. *Lancet*. 2023;402(10401):571–584. doi:10.1016/S0140-6736(23)00966-2
2. Zhang YZ, Li YY. Inflammatory bowel disease: pathogenesis. *World J Gastroenterol*. 2014;20(1):91–99. doi:10.3748/wjg.v20.i1.91
3. Wang S, Dong Z, Wan X. Global, regional, and national burden of inflammatory bowel disease and its associated anemia, 1990 to 2019 and predictions to 2050: an analysis of the global burden of disease study 2019. *Autoimmun Rev*. 2024;23(3):103498. doi:10.1016/j.autrev.2023.103498
4. Feuerstein JD, Cheifetz AS. Ulcerative colitis: epidemiology, diagnosis, and management. *Mayo Clin Proc*. 2014;89(11:1553–1563. doi:10.1016/j.mayocp.2014.07.002
5. Gajendran M, Loganathan P, Jimenez G, et al. A comprehensive review and update on ulcerative colitis. *Dis Mon*. 2019;65(12:100851. doi:10.1016/j.disamonth.2019.02.004
6. Kobayashi T, Siegmund B, Le Berre C, et al. Ulcerative colitis. *Nat Rev Dis Primers*. 2020;6(1):74. doi:10.1038/s41572-020-0205-x
7. Liu Y, Wu J, Tan L, et al. (-)-Syringaresinol attenuates ulcerative colitis by improving intestinal epithelial barrier function and inhibiting inflammatory responses. *Phytomedicine*. 2024;124:155292. doi:10.1016/j.phymed.2023.155292
8. Yin S, Yang H, Tao Y, et al. Artesunate ameliorates DSS-induced ulcerative colitis by protecting intestinal barrier and inhibiting inflammatory response. *Inflammation*. 2020;43(2):765–776. doi:10.1007/s10753-019-01164-1
9. Geremia A, Biancheri P, Allan P, Corazza GR, Di Sabatino A. Innate and adaptive immunity in inflammatory bowel disease. *Autoimmun Rev*. 2014;13(1:3–10. doi:10.1016/j.autrev.2013.06.004
10. Schirbel A, Fiocchi C. Inflammatory bowel disease: established and evolving considerations on its etiopathogenesis and therapy. *J Dig Dis*. 2010;11(5):266–276. doi:10.1111/j.1751-2980.2010.00449.x
11. Rosen CE, Palm NW. Navigating the microbiota seas: triangulation finds a way forward. *Cell Host Microbe*. 2018;23(1):1–3. doi:10.1016/j.chom.2017.12.015
12. Gkouskou KK, Deligianni C, Tsatsanis C, Eliopoulos AG. The gut microbiota in mouse models of inflammatory bowel disease. *Front Cell Infect Microbiol*. 2014;4:28. doi:10.3389/fcimb.2014.00028
13. Li H, Ye XF, Su YS, et al. Mechanism of acupuncture and moxibustion on promoting mucosal healing in ulcerative colitis. *Chin J Integr Med*. 2023;29(9:847–856. doi:10.1007/s11655-022-3531-x
14. Liu L, Dong W, Wang S, et al. Deoxycholic acid disrupts the intestinal mucosal barrier and promotes intestinal tumorigenesis. *Food Funct*. 2018;9(11):5588–5597. doi:10.1039/c8fo01143e
15. Cayrol C, Girard JP. IL-33: an alarmin cytokine with crucial roles in innate immunity, inflammation and allergy. *Curr Opin Immunol*. 2014;31:31–37. doi:10.1016/j.coi.2014.09.004
16. Liew FY, Pitman NI, McInnes IB. Disease-associated functions of IL-33: the new kid in the IL-1 family. *Nat Rev Immunol*. 2010;10(2):103–110. doi:10.1038/nri2692
17. Pastorelli L, Garg RR, Hoang SB, et al. Epithelial-derived IL-33 and its receptor ST2 are dysregulated in ulcerative colitis and in experimental Th1/Th2 driven enteritis. *Proc Natl Acad Sci U S A*. 2010;107(17:8017–8022. doi:10.1073/pnas.0912678107
18. Sedhom MA, Pichery M, Murdoch JR, et al. Neutralisation of the interleukin-33/ST2 pathway ameliorates experimental colitis through enhancement of mucosal healing in mice. *Gut*. 2013;62(12:1714–1723. doi:10.1136/gutjnl-2011-301785
19. Zhang Y, Xu C, Li F, Chen G. Notch/IL33/ST2 signaling was involved in the maintenance of intestinal epithelial barrier through regulating tight junction after LPS stimulation. *Cell Mol Biol*. 2025;71(2):36–42. doi:10.14715/cmb/2025.71.2.6
20. Chen J, He Y, Tu L, Duan L. Dual immune functions of IL-33 in inflammatory bowel disease. *Histol Histopathol*. 2020;35(2:137–146. doi:10.14670/HH-18-149
21. Eming SA, Wynn TA, Martin P. Inflammation and metabolism in tissue repair and regeneration. *Science*. 2017;356(6342):1026–1030. doi:10.1126/science.aam7928
22. He R, Yin H, Yuan B, et al. IL-33 improves wound healing through enhanced M2 macrophage polarization in diabetic mice. *Mol Immunol*. 2017;90:42–49. doi:10.1016/j.molimm.2017.06.249
23. Espinassous Q, Garcia-de-Paco E, Garcia-Verdugo I, et al. IL-33 enhances lipopolysaccharide-induced inflammatory cytokine production from mouse macrophages by regulating lipopolysaccharide receptor complex. *J Immunol*. 2009;183(2:1446–1455. doi:10.4049/jimmunol.0803067
24. Mosser DM, Edwards JP. Exploring the full spectrum of macrophage activation. Nat Rev Immunol. 2008 8(12):958-69. *Nat Rev Immunol*. 2010;10(6):460. (). doi:10.1038/nri2788
25. Isidro RA, Bonilla FJ, Pagan H, et al. The probiotic mixture VSL#3 alters the morphology and secretion profile of both polarized and unpolarized human macrophages in a polarization-dependent manner. *J Clin Cell Immunol*. 2014;5(3):1000227. doi:10.4172/2155-9899.1000227
26. Zhu W, Yu J, Nie Y, et al. Disequilibrium of M1 and M2 macrophages correlates with the development of experimental inflammatory bowel diseases. *Immunol Invest*. 2014;43(7:638–652. doi:10.3109/08820139.2014.909456
27. Lv Q, Xing Y, Liu Y, et al. Didymin switches M1-like toward M2-like macrophage to ameliorate ulcerative colitis via fatty acid oxidation. *Pharmacol Res*. 2021;169:105613. doi:10.1016/j.phrs.2021.105613

28. Fang Y, Zhao J, Chen Y, et al. Engineered nanoplatform with dual anti-inflammatory and microbiota-modulating actions for targeted therapy in chronic inflammatory bowel disease. *Small*. 2026;e10165. doi:10.1002/smll.202510165
29. Ma J, Zhang J, Wang Y, et al. Modified Gegen Qinlian decoction ameliorates DSS-induced chronic colitis in mice by restoring the intestinal mucus barrier and inhibiting the activation of γδT17 cells. *Phytomedicine*. 2023;111:154660. doi:10.1016/j.phymed.2023.154660
30. Wang Y, Zhang J, Zhang B, et al. Modified Gegen Qinlian decoction ameliorated ulcerative colitis by attenuating inflammation and oxidative stress and enhancing intestinal barrier function in vivo and in vitro. *J Ethnopharmacol*. 2023;313:116538. doi:10.1016/j.jep.2023.116538
31. Wang X, Huang S, Zhang M, et al. Gegen Qinlian decoction activates AhR/IL-22 to repair intestinal barrier by modulating gut microbiota-related tryptophan metabolism in ulcerative colitis mice. *J Ethnopharmacol*. 2023;302(Pt B:115919. doi:10.1016/j.jep.2022.115919
32. Zhao Y, Luan H, Jiang H, et al. Gegen Qinlian decoction relieved DSS-induced ulcerative colitis in mice by modulating Th17/Treg cell homeostasis via suppressing IL-6/JAK2/STAT3 signaling. *Phytomedicine*. 2021;84:153519. doi:10.1016/j.phymed.2021.153519
33. Hu Y, Tang J, Xie Y, et al. Gegen Qinlian decoction ameliorates TNBS-induced ulcerative colitis by regulating Th2/Th1 and Tregs/Th17 cells balance,inhibiting NLRP3 inflammasome activation and reshaping gut microbiota. J Ethnopharmacol. 2024 Jun 28;328:117956. *J Ethnopharmacol*. 2024;29;352:119788. doi:10.1016/j.jep.2025.119788
34. Lu JZ, Ye D, Ma BL. Constituents, pharmacokinetics, and pharmacology of Gegen-Qinlian decoction. *Front Pharmacol*. 2021;12:668418. doi:10.3389/fphar.2021.668418
35. Lu JZ, Hong DD, Ye D, et al. Tissue distribution and integrated pharmacokinetic properties of major effective constituents of oral Gegen-Qinlian decoction in mice. *Front Pharmacol*. 2022;13:996143. doi:10.3389/fphar.2022.996143
36. Tao Q, Liang Q, Fu Y, et al. Puerarin ameliorates colitis by direct suppression of macrophage M1 polarization in DSS mice. *Phytomedicine*. 2024;135:156048. doi:10.1016/j.phymed.2024.156048
37. Jeon YD, Lee JH, Lee YM, Kim DK. Puerarin inhibits inflammation and oxidative stress in dextran sulfate sodium-induced colitis mice model. *Biomed Pharmacother*. 2020;124:109847. doi:10.1016/j.biopha.2020.109847
38. Liu C, Li Y, Chen Y, et al. Baicalein restores the balance of Th17/Treg cells via aryl hydrocarbon receptor to attenuate colitis. *Mediators Inflamm*. 2020;2020:5918587. doi:10.1155/2020/5918587
39. Huang S, Fu Y, Xu B, et al. Wogonoside alleviates colitis by improving intestinal epithelial barrier function via the MLCK/pMLC2 pathway. *Phytomedicine*. 2020;68:153179. doi:10.1016/j.phymed.2020.153179
40. He L, Zhong Z, Liu F, Wen S. Berberine alleviates DSS-induced colitis by modulating macrophage phenotype via PPAR-γ/ mTOR/HIF-1α signaling pathway. *J Ethnopharmacol*. 2026;362:121350. doi:10.1016/j.jep.2026.121350
41. Wirtz S, Popp V, Kindermann M, et al. Chemically induced mouse models of acute and chronic intestinal inflammation. *Nat Protoc*. 2017;12 (7:1295–1309. doi:10.1038/nprot.2017.044
42. N NTP, Palmieri V, Adamczyk A, et al. IL-33 drives expansion of type 2 innate lymphoid cells and regulatory T cells and protects mice from severe, acute colitis. *Front Immunol*. 2021;12:669787. doi:10.3389/fimmu.2021.669787
43. Deng F, Hu JJ, Yang X, et al. Gut microbial metabolite pravastatin attenuates intestinal ischemia/reperfusion injury through promoting IL-13 release from type II innate lymphoid cells via IL-33/ST2 signaling. *Front Immunol*. 2021;12:704836. doi:10.3389/fimmu.2021.704836
44. Laroui H, Ingersoll SA, Liu HC, et al. Dextran sodium sulfate (DSS) induces colitis in mice by forming nano-lipocomplexes with medium-chain-length fatty acids in the colon. *PLoS One*. 2012;7(3:e32084. doi:10.1371/journal.pone.0032084
45. Xu J, Wu L, Yu P, Sun Y, Lu Y. Effect of T. spiralis Serine protease inhibitors on TNBS-induced experimental colitis mediated by Macrophages. *Sci Rep*. 2020;10(1):3147. doi:10.1038/s41598-020-60155-7
46. Sall IM, Vodnar DC, Martău GA, et al. Ethanolic extract of kinkeliba (combretum micranthum), rich in phenolic compounds mitigates DSS-induced ulcerative colitis in C57BL/6 mice via antioxidation and microbiota regulation. *Int J Mol Sci*. 2025;26(23):11299. doi:10.3390/ijms262311299
47. Lyu X, Zhang L, Si J, et al. Activation of the Nrf2 signaling pathway by a ginseng-salvia root-notoginseng composite alleviates ulcerative DSS-induced colitis via restoring gut microbiota and the intestinal barrier. *Antioxidants*. 2026;15(3):320. doi:10.3390/antiox15030320
48. Lu Y, Dai Y, Duan Y, et al. Fufang Tongye Shaoshang you repairs ulcerative colitis in mice caused by DSS based on the balanced strategy of "inflammation inhibition-microbiota regulation-mucosa protection". *J Ethnopharmacol*. 2026;367:121686. doi:10.1016/j.jep.2026.121686
49. Chen N, Luo S, Zhou X, et al. Sodium butyrate alleviates IBD by modulating SIRT1-involved ferroptosis and inhibition of macrophage ferroptosis. *Nutrients*. 2026;18(4):598. doi:10.3390/nu18040598
50. Yang C, Merlin D. Unveiling colitis: a journey through the dextran sodium sulfate-induced model. *Inflamm Bowel Dis*. 2024;30(5):844–853. doi:10.1093/ibd/izad312
51. Williams MA, O'Callaghan A, Corr SC. IL-33 and IL-18 in inflammatory bowel disease etiology and microbial interactions. *Front Immunol*. 2019;10:1091. doi:10.3389/fimmu.2019.01091
52. Andoh A, Nishida A. Pro- and anti-inflammatory roles of interleukin (IL)-33, IL-36, and IL-38 in inflammatory bowel disease. *J Gastroenterol*. 2023;58(2:69–78. doi:10.1007/s00535-022-01936-x
53. Beltrán CJ, Núñez LE, Díaz-Jiménez D, et al. Characterization of the novel ST2/IL-33 system in patients with inflammatory bowel disease. *Inflamm Bowel Dis*. 2010;16(7):1097–1107. doi:10.1002/ibd.21175
54. Díaz-Jiménez D, De la Fuente M, Dubois-Camacho K, et al. Soluble ST2 is a sensitive clinical marker of ulcerative colitis evolution. *BMC Gastroenterol*. 2016;16(1):103. doi:10.1186/s12876-016-0520-6
55. Chang YJ, Kim HY, Albacker LA, et al. Innate lymphoid cells mediate influenza-induced airway hyper-reactivity independently of adaptive immunity. *Nat Immunol*. 2011;12(7):631–638. doi:10.1038/ni.2045
56. Monticelli LA, Sonnenberg GF, Abt MC, et al. Innate lymphoid cells promote lung-tissue homeostasis after infection with influenza virus. *Nat Immunol*. 2011;12(11):1045–1054. doi:10.1031/ni.2131
57. Matta BM, Reichenbach DK, Zhang X, et al. Peri-alloHCT IL-33 administration expands recipient T-regulatory cells that protect mice against acute GVHD. *Blood*. 2016;128(3:427–439. doi:10.1182/blood-2015-12-684142
58. Arpaia N, Green JA, Moltedo B, et al. A distinct function of regulatory T cells in tissue protection. *Cell*. 2015;162(5):1078–1089. doi:10.1016/j.cell.2015.08.021
59. Burzyn D, Kuswanto W, Kolodin D, et al. A special population of regulatory T cells potentiates muscle repair. *Cell*. 2013;155(6):1282–1295. doi:10.1016/j.cell.2013.10.054

60. Zaiss DMW, Gause WC, Osborne LC, Artis D. Emerging functions of amphiregulin in orchestrating immunity, inflammation, and tissue repair. *Immunity*. 2015;42(2):216–226. doi:10.1016/j.immuni.2015.01.020
61. Bonilla WV, Fröhlich A, Senn K, et al. The alarmin interleukin-33 drives protective antiviral $CD8^+$ T cell responses. *Science*. 2012;335 (6071:984–989. doi:10.1126/science.1215418
62. Reichenbach DK, Schwarze V, Matta BM, et al. The IL-33/ST2 axis augments effector T-cell responses during acute GVHD. Blood. 2015;125(20):3183-92. *Blood*. 2016;128(9):1311. doi:10.1182/blood-2016-07-728048
63. Yang Q, Li G, Zhu Y, et al. IL-33 synergizes with TCR and IL-12 signaling to promote the effector function of CD8+ T cells. *Eur J Immunol*. 2011;41(11:3351–3360. doi:10.1002/eji.201141629
64. Gao X, Wang X, Yang Q, et al. Tumoral expression of IL-33 inhibits tumor growth and modifies the tumor microenvironment through CD8+ T and NK cells. *J Immunol*. 2015;194(1:438–445. doi:10.4049/jimmunol.1401344
65. Baumann C, Bonilla WV, Fröhlich A, et al. T-bet- and STAT4-dependent IL-33 receptor expression directly promotes antiviral Th1 cell responses. *Proc Natl Acad Sci USA*. 2015;112(13:4056–4061. doi:10.1073/pnas.1418549112
66. Smithgall MD, Comeau MR, Yoon BR, Kaufman D, Armitage R, Smith DE. IL-33 amplifies both Th1- and Th2-type responses through its activity on human basophils, allergen-reactive Th2 cells, iNKT and NK cells. *Int Immunol*. 2008;20(8:1019–1030. doi:10.1093/intimm/dxn060
67. Kearley J, Silver JS, Sanden C, et al. Cigarette smoke silences innate lymphoid cell function and facilitates an exacerbated type I interleukin-33-dependent response to infection. *Immunity*. 2015;42(3):566–579. doi:10.1016/j.immuni.2015.02.011
68. Bourgeois E, Van LP, Samson M, et al. The pro-Th2 cytokine IL-33 directly interacts with invariant NKT and NK cells to induce IFN-gamma production. *Eur J Immunol*. 2009;39(4):1046–1055. doi:10.1002/eji.200838575
69. Kobori A, Yagi Y, Imaeda H, et al. Interleukin-33 expression is specifically enhanced in inflamed mucosa of ulcerative colitis. *J Gastroenterol*. 2010;45(10:999–1007. doi:10.1007/s00535-010-0245-1
70. Sponheim J, Pollheimer J, Olsen T, et al. Inflammatory bowel disease-associated interleukin-33 is preferentially expressed in ulceration-associated myofibroblasts. *Am J Pathol*. 2010;177(6:2804–2815. doi:10.2353/ajpath.2010.100378
71. Gundersen MD, Goll R, Hol J, et al. Loss of interleukin 33 expression in colonic crypts - a potential marker for disease remission in ulcerative colitis. *Sci Rep*. 2016;6:35403. doi:10.1038/srep35403
72. Oboki K, Ohno T, Kajiwara N, et al. IL-33 is a crucial amplifier of innate rather than acquired immunity. *Proc Natl Acad Sci U S A*. 2010;107 (43:18581–18586. doi:10.1073/pnas.1003059107
73. Kayamuro H, Yoshioka Y, Abe Y, et al. Interleukin-1 family cytokines as mucosal vaccine adjuvants for induction of protective immunity against influenza virus. *J Virol*. 2010;84(24:12703–12712. doi:10.1128/JVI.01182-10
74. Hu J, Gao N, Zhang Y, et al. IL-33/ST2/IL-9/IL-9R signaling disrupts ocular surface barrier in allergic inflammation. *Mucosal Immunol*. 2020;13 (6:919–930. doi:10.1038/s41385-020-0288-4
75. Jin J, Fan YJ, Nguyen TV, et al. Chaenomeles sinensis extract ameliorates ovalbumin-induced allergic rhinitis by inhibiting the IL-33/ST2 axis and regulating epithelial cell dysfunction. *Foods*. 2024;13(4):611. doi:10.3390/foods13040611
76. Kotsiou OS, Gourgoulianis KI, Zarogiannis SG. IL-33/ST2 axis in organ fibrosis. *Front Immunol*. 2018;9:2432. doi:10.3389/fimmu.2018.02432
77. Xu Z, Zhao C, Wang Z, et al. Interleukin-33 levels are elevated in chronic allograft dysfunction of kidney transplant recipients and promotes epithelial to mesenchymal transition of human kidney (HK-2) cells. *Gene*. 2018;644:113–121. doi:10.1016/j.gene.2017.11.010
78. Murray PJ, Wynn TA. Protective and pathogenic functions of macrophage subsets. *Nat Rev Immunol*. 2011;11(11):723–737. doi:10.1038/nri3073
79. Yunna C, Mengru H, Lei W, Weidong C. Macrophage M1/M2 polarization. *Eur J Pharmacol*. 2020;877:173090. doi:10.1016/j.ejphar.2020.173090
80. Bain CC, Schridde A. Origin, differentiation, and function of intestinal macrophages. *Front Immunol*. 2018;9:2733. doi:10.3389/fimmu.2018.02733
81. Luiz JPM, Toller-Kawahisa JE, Viacava PR, et al. MEK5/ERK5 signaling mediates IL-4-induced M2 macrophage differentiation through regulation of c-Myc expression. *J Leukoc Biol*. 2020;108(4):1215–1223. doi:10.1002/JLB.1MA0520-016R
82. Hidalgo-Garcia L, Galvez J, Rodriguez-Cabezas ME, Anderson PO. Can a conversation between mesenchymal stromal cells and macrophages solve the crisis in the inflamed intestine? *Front Pharmacol*. 2018;9:179. doi:10.3389/fphar.2018.00179
83. Philippidis P, Mason JC, Evans BJ, et al. Hemoglobin scavenger receptor CD163 mediates interleukin-10 release and heme oxygenase-1 synthesis: antiinflammatory monocyte-macrophage responses in vitro, in resolving skin blisters in vivo, and after cardiopulmonary bypass surgery. *Circ Res*. 2004;94(1:119–126. doi:10.1161/01.RES.0000109414.78907.F9
84. Van Gorp H, Delputte PL, Nauwynck HJ. Scavenger receptor CD163, a Jack-of-all-trades and potential target for cell-directed therapy. *Mol Immunol*. 2010;47(7–8):1650–1660. doi:10.1016/j.molimm.2010.02.008
85. Cayrol C, Girard JP. Interleukin-33 (IL-33): a nuclear cytokine from the IL-1 family. *Immunol Rev*. 2018;281(1):154–168. doi:10.1111/imr.12619
86. Chen Z, Xu Y, Qu C, et al. The IL-33/ST2 axis promotes traumatic heterotopic ossification by driving macrophage and mast cell-mediated inflammation via autophagy defects. *Int J Biol Sci*. 2026;22(1):60–85. doi:10.7150/ijbs.122706
87. Yasen A, Tang Y, Yang X, et al. IL-33/ST2 signaling promotes intrahepatic cholangiocarcinoma through reprogramming macrophage polarization via MAPK pathway. *Exp Cell Res*. 2026;455(1:114845. doi:10.1016/j.yexcr.2025.114845
88. Faas M, Ipseiz N, Ackermann J, et al. IL-33-induced metabolic reprogramming controls the differentiation of alternatively activated macrophages and the resolution of inflammation. *Immunity*. 2021;54(11:2531–2546.e5. doi:10.1016/j.immuni.2021.09.010
89. Xu H, Sun L, He Y, et al. Deficiency in IL-33/ST2 axis reshapes mitochondrial metabolism in lipopolysaccharide-stimulated macrophages. *Front Immunol*. 2019;10:127. doi:10.3389/fimmu.2019.00127
90. Wan X, Zhang C, Lei P, et al. Precision therapeutics for inflammatory bowel disease: advancing ROS-responsive nanoparticles for targeted and multifunctional drug delivery. *J Mater Chem B*. 2025;13(10):3245–3269. doi:10.1039/d4tb02868f
91. Lin C, Zhou Z, Zhang L, et al. Gegen Qinlian decoction relieves ulcerative colitis via adjusting dysregulated Nrf2/ARE signaling. *Evid Based Complement Alternat Med*. 2022;2934552. doi:10.1155/2022/2934552
92. Huang J, Zhang J, Liu Z, et al. Modified Gegen Qinlian decoction ameliorates DSS-induced colitis in mice via the modulation of NF-κB and Nrf2/HO-1 pathways. *Mediators Inflamm*. 2025;2025:7468297. doi:10.1155/mi/7468297